PTEP
Prog. Theor. Exp. Phys. **2020**, 123B01 (20 pages)
DOI: 10.1093/ptep/ptaa150

# Scalar clockwork and flavor neutrino mass matrix

Teruyuki Kitabayashi*

*Department of Physics, Tokai University, 4-1-1 Kitakaname, Hiratsuka, Kanagawa 259-1292, Japan*
*E-mail: teruyuki@tokai-u.jp

Received September 8, 2020; Revised October 3, 2020; Accepted October 4, 2020; Published December 10, 2020

We study the capability of generating the correct flavor neutrino mass matrix in a scalar clockwork model. First, we assume that the flavor structure is controlled by the Yukawa couplings as in the standard model. In this case, the correct flavor neutrino mass matrix could be obtained by appropriate Yukawa couplings $Y_{\ell'\ell}$ where $\ell', \ell = e, \mu, \tau$. Next, we assume that the Yukawa couplings are extremely democratic: $|Y_{\ell'\ell}| = 1$. In this case, the model parameters of the scalar clockwork sector, such as the site number of a clockwork gear in a clockwork chain, should have the flavor indices $\ell'$ and/or $\ell$ to generate the correct flavor neutrino mass matrix. We show some examples of assignments of the flavor indices which can yield the correct flavor neutrino mass matrix.

Subject Index B40, B54

## 1. Introduction

Understanding the nature of the tiny neutrino masses as well as their mixings is one of the outstanding problems in particle physics and cosmology [1]. Many theoretical mechanisms to generate tiny neutrino masses have been proposed, such as seesaw mechanisms [2–5], radiative mechanisms [6–13], and the scotogenic model [14]. On the other hand, the neutrino mixings have been studied under assumptions of the existence of underlying flavor symmetries in the theories (for reviews, see Refs. [15–17]). Apart from the neutrino problems, there are many mysteries related to the hierarchy in particle physics.

The clockwork mechanism [18] provides a natural way to obtain the hierarchical masses and couplings in a theory. The basic idea of the clockwork mechanism is simple [19]. A product

$$\frac{1}{q} \times \frac{1}{q} \times \cdots \times \frac{1}{q}, \tag{1}$$

with $q > 1$, can become tiny if the number of factors is increased. There is an analogy between the series of gears in a clock and this product. In a series of gears, a large (small) movement of a gear on one side of the series can generate a small (large) movement of the gear on the opposite side. The factor $1/q$ behaves like a clockwork gear and the product behaves like a series of gears.

To implement this idea in quantum field theory, a large number of fields $\phi_i$ are introduced into a theory as the clockwork gears. These fields interact with the standard model (SM) particles schematically as

$$\phi_0 \underset{\frac{1}{q}}{-} \phi_1 \underset{\frac{1}{q}}{-} \cdots \underset{\frac{1}{q}}{-} \phi_N - \mathrm{SM}, \tag{2}$$

with couplings $1/q \lesssim 1$, where $N$ denotes the number of gears. The series of fields behaves like a clockwork chain. If one of the mass eigenstates (typically the lightest state) $\phi_{\rm light}$ is essentially given


Funded by SCOAP³

by $\phi_0$, the interaction between $\phi_{\text{light}}$ and the standard model particles will be suppressed as

$$\phi_{\text{light}} - \text{SM} \sim \frac{1}{q^N} \tag{3}$$

for large $N$. Therefore, we can obtain a tiny coupling $1/X$ by $\mathcal{O}(1)$ couplings $1/q$ and a large number of fields $N \sim \log_q X$. This is the outline of the scalar clockwork mechanism. The basics of other clockwork mechanisms, such as the fermion clockwork mechanism, are essentially the same as the basics of the scalar clockwork mechanism.

Applications of the clockwork mechanism have been extensively studied in the literature, e.g. for the axion [20–29], for inflation [30,31], for dark matter [32–36], for the $g-2$ muon [37], for string theory [38–40], for gravity [41,42], for grand unified theories [44,45], for charged fermion masses and mixings [43], for quark masses and mixings [46], and for Goldstone bosons [47].

Applications of the clockwork mechanism to the neutrino sector have been studied for tiny neutrino masses [48–50] and for their mixings [51,52]. Up to now, there are two fermion clockwork models for the neutrino mixings [51,52]; however, there is no scalar clockwork model for the neutrino mixings.

In this paper, towards a construction of scalar clockwork models including neutrino mixings, we extend the scalar clockwork model proposed by Banerjee, Ghosh, and Ray [49] for a one-generation neutrino (without mixing) to a model for three-generation neutrinos (with mixings). Since any correct scalar clockwork models for three-generation neutrinos should yield a $3 \times 3$ flavor neutrino mass matrix which is consistent with observations, we would like to concentrate our discussion on the mathematical capability of generating a correct flavor neutrino mass matrix.

The paper is organized as follows. In Sect. 2 we present a brief review of scalar clockwork mechanisms. In Sect. 3, towards a construction of scalar clockwork models including neutrino mixings, we study the mathematical capability of generating a correct flavor neutrino mass matrix in a scalar clockwork model. Section 4 is devoted to a summary.

## 2. Review of scalar clockwork

### *2.1. Scalar clockwork mechanism*

The total Lagrangian of the standard model with the clockwork sector reads

$$\mathcal{L} = \mathcal{L}_{\text{SM}} + \mathcal{L}_{\text{CW}} + \mathcal{L}_{\text{SM}-\text{CW}}, \tag{4}$$

where $\mathcal{L}_{\text{SM}}$ denotes the standard model Lagrangian, $\mathcal{L}_{\text{CW}}$ denotes the interactions in the clockwork sector, and $\mathcal{L}_{\text{SM}-\text{CW}}$ denotes the interactions between the standard model sector and the clockwork sector.

In scalar clockwork models there are $N+1$ scalars, $\Phi_j$ ($j = 0, 1, \ldots, N$), with $N+1$ global U(1) symmetries. These U(1) symmetries are spontaneously broken to their discrete subgroups $\text{Z}_2$ at some scale $f$. The clockwork Lagrangian can be written as [18,49]

$$\mathcal{L}_{\text{CW}} = \sum_{j=0}^{N} \left[ \partial_\mu \Phi_j^\dagger \partial^\mu \Phi_j - \frac{\lambda}{8} (\Phi_j^\dagger \Phi_j - f^2)^2 \right] + \frac{1}{2} \Lambda^{3-q} \sum_{j=0}^{N-1} \left( \Phi_j^\dagger \Phi_{j+1}^q + \text{h.c.} \right), \tag{5}$$

where $q \in \mathbb{Z}$ and $j \in \mathbb{N}$ [47]. The first two terms in Eq. (5) are invariant under the global $\text{U}(1)^{N+1}$; on the other hand, the last term breaks the symmetry down to a single remnant $\text{U}(1)_{\text{CW}}$. The explicit breaking term is renormalizable and soft ($\Lambda \ll f$) if $1 < q \leq 3$ is satisfied [22,49]. Since $q \in \mathbb{Z}$, the requirement of

$$q = 2, 3 \tag{6}$$

should be satisfied in the scalar clockwork models described by the Lagrangian in Eq. (5). Sometimes, the requirements of $q \in \mathbb{N}$ and $j \in \mathbb{N}$ are relaxed in the analysis (see, for examples, Ref. [34]); however, we would like to keep the requirements of Eq. (6) and $j \in \mathbb{N}$ in the main part of this paper.

After the spontaneous symmetry breaking, the effective fields are $N+1$ Nambu–Goldstone (NG) bosons $\pi_j$ that can be conveniently described by

$$U_j = e^{i\pi_j/f}. \tag{7}$$

The explicit breaking term in $\mathcal{L}_{\mathrm{CW}}$ is not invariant under the shift symmetries of the NG bosons ($\pi_j \to \pi_j + \alpha_j$). On the other hand, the remnant unbroken $\mathrm{U}(1)_{\mathrm{CW}}$ is invariant under the transformation

$$\pi_j \to \pi_j + \frac{\alpha}{q^{j-1}}, \qquad j = 0, \ldots, N. \tag{8}$$

The unbroken $\mathrm{U}(1)_{\mathrm{CW}}$ corresponds to the generator

$$Q = \sum_{j=0}^{N} \frac{Q_j}{q^j}, \tag{9}$$

where $Q_j$ is the generator of $j$th site.

In terms of the fields $\pi_j$, we obtain the pseudo-NG boson potential [49]

$$\begin{aligned} V_\pi &= -\frac{1}{2} f^{q-1} \Lambda^{3-q} \sum_{j=0}^{N-1} \left( U_j^\dagger U_{j+1}^q + \text{h.c.} \right) \\ &= -f^{q-1} \Lambda^{3-q} \sum_{j=0}^{N-1} \cos\left( \frac{\pi_j - q\pi_{j+1}}{f} \right) \\ &= -\frac{1}{2} \sum_{i,j=0}^{N} \pi_i (M_\pi^2)_{ij} \pi_j + \mathcal{O}(\pi^4). \end{aligned} \tag{10}$$

The mass matrix is given by

$$M_\pi^2 = f^{q-1} \Lambda^{3-q} \begin{pmatrix} 1 & -q & 0 & \cdots & 0 & 0 \\ -q & q^2+1 & -q & \cdots & 0 & 0 \\ 0 & -q & q^2+1 & \cdots & 0 & 0 \\ \vdots & \vdots & \vdots & \ddots & \vdots & \vdots \\ 0 & 0 & 0 & & q^2+1 & -q \\ 0 & 0 & 0 & \cdots & -q & q^2 \end{pmatrix}. \tag{11}$$

The tridiagonal symmetric mass matrix $M_\pi^2$ can be diagonal by the orthogonal rotation

$$\pi_j = \mathcal{O}_{jk} a_k, \qquad (j = 0, \ldots, N,\ k = 1, \ldots, N), \tag{12}$$

where

$$\mathcal{O}_{j0} = \frac{1}{q^j}\sqrt{\frac{q^2-1}{q^2-q^{-2N}}},$$
$$\mathcal{O}_{jk} = \sqrt{\frac{2}{(N+1)\lambda_k}}\left[q\sin\frac{jk\pi}{N+1} - q\sin\frac{(j+1)k\pi}{N+1}\right], \tag{13}$$

with

$$\lambda_k = q^2+1-2q\cos\frac{k\pi}{N+1}. \tag{14}$$

After the rotation, one massless eigenvalue of the one massless NG mode $a_0$ and $N$ massive eigenvalues for $N$ massive pseudo-NG modes $a_k$ are obtained as

$$m_{a_0}^2 = 0, \qquad m_{a_k}^2 = \lambda_k f^{q-1}\Lambda^{3-q}, \quad (k=1,\ldots,N). \tag{15}$$

$\mathcal{O}_{j0}$ in Eq. (13) measures the component of the massless NG state contained in $\pi_j$. Since $\mathcal{O}_{j0} \propto q^{-j}$, the NG state $a_0 = \mathcal{O}_{j0}\pi_j$ is $q$ times smaller than for the previous site. Thus, the NG interaction may be secluded away from the last side for large $N$. If standard model fields are coupled to the clockwork sector only through its $N$th site, the massless eigenstate $a_0$ is hierarchically localized at the different sites with a factor $1/q^j$ and can give rise to an exponential suppression. This is the scalar clockwork mechanism.

### 2.2. *Scalar clockwork and one-flavor neutrino*

A way to generate the tiny neutrino mass by the scalar clockwork mechanism for one-flavor neutrino was proposed by Banerjee, Ghosh, and Ray [49]. They applied a *clockworked vacuum expectation values* (VEVs) mechanism to a simple model to explain the tiny neutrino mass.

The NG bosons arising in $V_\pi$ possess a discrete $Z_2$ symmetry and cannot receive VEVs. In the clockworked VEVs mechanism, to generate a hierarchical VEV structure an additional soft breaking potential ($\mu_1, \mu_2 \ll f$)

$$\begin{aligned} V_{\rm soft} &= -\frac{\mu_1^2 f^2}{4}(U_k + \text{h.c.})^2 + \frac{\mu_2^3 f}{2}(iU_k + \text{h.c.}) \\ &= -\mu_1^2 f^2\cos^2\frac{\pi_k}{f} - \mu_2^3 f\sin\frac{\pi_k}{f} \end{aligned} \tag{16}$$

is introduced for the $k$th site to break the residual $U(1)_{\rm CW}$ as well as $Z_2$ symmetry explicitly. If the breaking potential is added at zeroth site, $k=0$, the minimization condition for the total potential $V = V_\pi + V_{\rm soft}$ yields

$$\langle\pi_0\rangle = \frac{\mu_2^3}{2\mu_1^2} \tag{17}$$

and

$$\langle\pi_1\rangle = \frac{\langle\pi_0\rangle}{q},\ \langle\pi_2\rangle = \frac{\langle\pi_0\rangle}{q^2},\ \ldots,\ \langle\pi_N\rangle = \frac{\langle\pi_0\rangle}{q^N}. \tag{18}$$

The VEV arising at the farthest end (the $N$th site) from the soft-breaking site (the 0th site) may be small for large $q^N$. This is the clockworked VEVs mechanism.

A simple model for a one-generation neutrino can be obtained as follows. According to Banerjee et al., we assume that the right-handed neutrino $\nu_R$ possesses a charge under the $Z_2$ symmetry of the $j$th site of the clockwork chain, denoted by $Z_2^{(j)}$. The $Z_2^{(j)}$ charges are assigned as $Z_2^{(j)}(\pi_j) = Z_2^{(j)}(\nu_R) = -1$ and $Z_2^{(j)}(\text{others}) = +1$. In this case, the interaction between the clockwork sector and the right-handed neutrino will be, schematically,

$$\begin{array}{c} \pi_0 - \pi_1 - \pi_2 - \cdots - \pi_j - \cdots - \pi_N \\ | \\ \nu_R \end{array} \tag{19}$$

This phenomenon is described by the following interaction Lagrangian:

$$\mathcal{L}_{\mathrm{SM-CW}} = y\left(\frac{\pi_j}{f}\right)\bar{\ell}_L\tilde{H}\nu_R + \text{h.c.}, \tag{20}$$

where $y$ denotes some effective coupling, $\ell_L$ denotes the standard model left-handed lepton doublet, and $H$ denotes the standard model Higgs doublet. After symmetry breaking, the fields obtain the VEV

$$\begin{array}{c} \langle\pi_0\rangle - \dfrac{\langle\pi_0\rangle}{q} - \dfrac{\langle\pi_0\rangle}{q^2} - \cdots - \dfrac{\langle\pi_0\rangle}{q^j} - \cdots - \dfrac{\langle\pi_0\rangle}{q^N} \\ | \\ \nu_R \end{array} \tag{21}$$

and the Dirac mass of the neutrino is obtained as

$$m_\nu = \frac{yv}{\sqrt{2}}\frac{\langle\pi_j\rangle}{f} \simeq \frac{yv}{\sqrt{2}}\left(\frac{\langle\pi_0\rangle}{f}\frac{1}{q^j}\right) = \frac{yv^{\mathrm{eff}}}{\sqrt{2}}, \tag{22}$$

where $v$ denotes the VEV of the Higgs and $v^{\mathrm{eff}}$ denotes an effective VEV. The effective VEV

$$v^{\mathrm{eff}} = v\left(\frac{\langle\pi_0\rangle}{f}\frac{1}{q^j}\right) \tag{23}$$

may be tiny for large $q^j$ by the clockworked VEVs mechanism, and the tiny neutrino mass may be generated. For example, assuming

$$y \sim \mathcal{O}(1), \qquad \frac{\langle\pi_0\rangle}{f} \sim \mathcal{O}(0.1), \qquad q = 3, \tag{24}$$

we find the tiny neutrino mass $m_\nu \sim 0.1$ eV if the right-handed neutrino couples to the 24th site ($j = 24$) of the clockwork chain.

## 3. Flavor neutrino mass matrix

### *3.1. Experimental constraints*

We show the basics of the flavor neutrino mass matrix and the constraints on the mass matrix from observations.

The flavor neutrino mass matrix

$$M = \begin{pmatrix} M_{ee} & M_{e\mu} & M_{e\tau} \\ M_{\mu e} & M_{\mu\mu} & M_{\mu\tau} \\ M_{\tau e} & M_{\tau\mu} & M_{\tau\tau} \end{pmatrix} \tag{25}$$

satisfies the relation

$$MM^\dagger = U_{\rm PMNS} \begin{pmatrix} m_1^2 & 0 & 0 \\ 0 & m_2^2 & 0 \\ 0 & 0 & m_3^2 \end{pmatrix} U_{\rm PMNS}^\dagger, \tag{26}$$

where $m_1$, $m_2$, and $m_3$ denote the neutrino mass eigenstates and

$$U_{\rm PMNS} = \begin{pmatrix} c_{12}c_{13} & s_{12}c_{13} & s_{13} \\ -s_{12}c_{23} - c_{12}s_{23}s_{13} & c_{12}c_{23} - s_{12}s_{23}s_{13} & s_{23}c_{13} \\ s_{12}s_{23} - c_{12}c_{23}s_{13} & -c_{12}s_{23} - s_{12}c_{23}s_{13} & c_{23}c_{13} \end{pmatrix}$$

denotes the mixing matrix [53]. We use the abbreviations $c_{ij} = \cos\theta_{ij}$ and $s_{ij} = \sin\theta_{ij}$ ($i,j$=1,2,3) and ignore the CP-violating phase.

Although the neutrino mass ordering (either the normal mass ordering or the inverted mass ordering) is not determined, a global analysis shows that the preference for the normal mass ordering is mostly due to neutrino oscillation measurements [54]. Upcoming experiments for neutrinos will be solve this problem [55]. In this paper we assume the normal mass hierarchical spectrum for the neutrinos, e.g. $m_1 < m_2 < m_3$. The best-fit values of the squared mass differences $\Delta m_{ij}^2 = m_i^2 - m_j^2$ and the mixing angles (as well as $1\,\sigma$ and $3\,\sigma$ allowed regions) are estimated as [56][1]

$$\begin{aligned}
\frac{\Delta m_{21}^2}{10^{-5}\,{\rm eV}^2} &= 7.39^{+0.21}_{-0.20} \qquad (6.79 \to 8.01), \\
\frac{\Delta m_{31}^2}{10^{-3}\,{\rm eV}^2} &= 2.528^{+0.029}_{-0.031} \qquad (2.436 \to 2.618), \\
\theta_{12}/^\circ &= 33.82^{+0.78}_{-0.76} \qquad (31.61 \to 36.27), \\
\theta_{23}/^\circ &= 48.6^{+1.0}_{-1.4} \qquad (41.1 \to 51.3), \\
\theta_{13}/^\circ &= 8.60^{+0.13}_{-0.13} \qquad (8.22 \to 8.98),
\end{aligned}$$

where $\pm$ denotes the $1\,\sigma$ region and the parentheses denote the $3\,\sigma$ region.

In this paper we will use the following experimental constraints on the flavor neutrino mass matrix: (A) Best-fit values: The flavor neutrino mass matrix should be

$$M = \begin{pmatrix} 0.821m_1 & 0.550m_2 & 0.150m_3 \\ -0.461m_1 & 0.487m_2 & 0.742m_3 \\ 0.335m_1 & -0.678m_2 & 0.654m_3 \end{pmatrix} \tag{27}$$

for the best-fit values of the neutrino oscillation parameters, where

$$m_2 = \sqrt{7.39 \times 10^{-5} + m_1^2}\ {\rm eV}, \qquad m_3 = \sqrt{2.528 \times 10^{-3} + m_1^2}\ {\rm eV} \tag{28}$$

for $m_1$. We will use

$$M = \begin{pmatrix} 0.0821 & 0.0552 & 0.0617 \\ -0.0461 & 0.0489 & 0.0831 \\ 0.0335 & -0.0681 & 0.0732 \end{pmatrix} {\rm eV} \tag{29}$$

for $m_1 = 0.1$ eV as a benchmark of the correct flavor neutrino mass matrix with the best-fit values of the neutrino parameters.

[1] See also the NuFIT webpage, http://www.nu-fit.org.

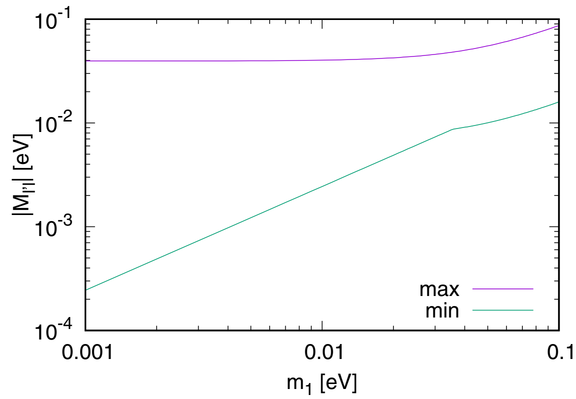


**Fig. 1.** The allowed region of the flavor neutrino masses $|M_{\ell'\ell}|$ ($\ell', \ell = e, \mu, \tau$) in the $3\,\sigma$ region. The upper and lower curves show the maximum and minimum magnitudes of the flavor neutrino masses, respectively. The allowed region becomes wide (narrow) for small (large) $m_1$.

(B) $3\,\sigma$ region: Figure 1 shows the allowed region of the magnitude of the flavor neutrino masses $|M_{\ell'\ell}|$ ($\ell', \ell = e, \mu, \tau$) in the $3\,\sigma$ region. The upper and lower curves show the maximum and minimum magnitudes of the flavor neutrino masses, respectively. The allowed region becomes wide for small $m_1$ and narrow for large $m_1$. We will use

$$|M_{\ell'\ell}| = \begin{cases} 0.000244 - 0.0395\,\mathrm{eV} & (m_1 = 0.001\,\mathrm{eV}), \\ 0.00244 - 0.0403\,\mathrm{eV} & (m_1 = 0.01\,\mathrm{eV}), \\ 0.0159 - 0.0868\,\mathrm{eV} & (m_1 = 0.1\,\mathrm{eV}), \end{cases} \tag{30}$$

as well as

$$\begin{pmatrix} |M_{ee}| & |M_{e\mu}| & |M_{e\tau}| \\ |M_{\mu e}| & |M_{\mu\mu}| & |M_{\mu\tau}| \\ |M_{\tau e}| & |M_{\tau\mu}| & |M_{\tau\tau}| \end{pmatrix} = \begin{pmatrix} 0.000796 - 0.000843 & 0.00430 - 0.00527 & 0.00706 - 0.00799 \\ 0.000423 - 0.000529 & 0.00359 - 0.00534 & 0.0321 - 0.0395 \\ 0.000244 - 0.000390 & 0.00493 - 0.00645 & 0.0305 - 0.0382 \end{pmatrix} \mathrm{eV}, \tag{31}$$

for $m_1 = 0.001$ eV,

$$\begin{pmatrix} |M_{ee}| & |M_{e\mu}| & |M_{e\tau}| \\ |M_{\mu e}| & |M_{\mu\mu}| & |M_{\mu\tau}| \\ |M_{\tau e}| & |M_{\tau\mu}| & |M_{\tau\tau}| \end{pmatrix} = \begin{pmatrix} 0.00796 - 0.00843 & 0.00671 - 0.00786 & 0.00720 - 0.00814 \\ 0.00423 - 0.00529 & 0.00560 - 0.00795 & 0.0327 - 0.0403 \\ 0.00244 - 0.00390 & 0.00769 - 0.00961 & 0.0311 - 0.0389 \end{pmatrix} \mathrm{eV}, \tag{32}$$

for $m_1 = 0.01$ eV, and

$$\begin{pmatrix} |M_{ee}| & |M_{e\mu}| & |M_{e\tau}| \\ |M_{\mu e}| & |M_{\mu\mu}| & |M_{\mu\tau}| \\ |M_{\tau e}| & |M_{\tau\mu}| & |M_{\tau\tau}| \end{pmatrix}$$
$$= \begin{pmatrix} 0.0796-0.0843 & 0.0519-0.0588 & 0.0159-0.0175 \\ 0.0423-0.0529 & 0.0433-0.0595 & 0.0724-0.0868 \\ 0.0244-0.0390 & 0.0596-0.0719 & 0.0689-0.0838 \end{pmatrix} \text{eV}, \tag{33}$$

for $m_1 = 0.1$ eV as the benchmarks of the correct flavor neutrino masses in the $3\,\sigma$ region.

### 3.2. *Yukawa dominant*

As we saw in the previous section, the tiny neutrino mass can be generated by clockworked VEVs mechanisms without neutrino mixing.

Now we extend the clockworked VEVs model for a one-generation neutrino (without mixing) to a model for three-generation neutrinos (with mixings). As we mentioned in Sect. 1, since any correct scalar clockwork model for three-generation neutrinos should yield a $3 \times 3$ neutrino flavor mass matrix which is consistent with observations, we would like to concentrate our discussion on the mathematical capability of generating the correct flavor neutrino mass matrix.

To reproduce the mixings between three Dirac neutrino flavors, the non-diagonal Yukawa matrix elements $Y_{\ell'\ell}$ $(\ell', \ell = e, \nu, \tau)$ should be included in the model. As the simplest extension of Eq. (20), we just change one right-handed neutrino $\nu_R$ to three right-handed neutrinos $\nu_{\ell R}$ $(\ell = e, \nu, \tau)$ and the single Yukawa coupling $y$ to the nine Yukawa couplings $Y_{\ell'\ell}$. The extended model then has the following interaction Lagrangian:

$$\mathcal{L}_{\text{SM}-\text{CW}} = \sum_{\ell',\ell} Y_{\ell'\ell} \left(\frac{\pi_j}{f}\right) \bar{\ell}'_L \tilde{H} \nu_{\ell R} + \text{h.c.} \tag{34}$$

The tiny elements of the flavor neutrino mass matrix

$$M_{\ell'\ell} \simeq Y_{\ell'\ell} \frac{v}{\sqrt{2}} \left(\frac{\langle\pi_0\rangle}{f} \frac{1}{q^j}\right) = Y_{\ell'\ell} \frac{v^{\text{eff}}}{\sqrt{2}} \tag{35}$$

are obtained by the clockworked VEVs mechanism where the effective VEV, $v^{\text{eff}}$, is the same as Eq. (23).

The correct neutrino masses and mixings are obtained by an appropriate Yukawa matrix as in the standard model. For example, the Yukawa matrix

$$Y = \begin{pmatrix} 1.33 & 0.896 & 0.272 \\ -0.748 & 0.793 & 1.35 \\ 0.544 & -1.10 & 1.19 \end{pmatrix} \tag{36}$$

and

$$\frac{\langle\pi_0\rangle}{f} = 0.1, \qquad q = 3, \qquad j = 24 \tag{37}$$

yield the flavor neutrino mass matrix in Eq. (29), which is consistent with the best-fit values of neutrino oscillation parameters for $m_1 = 0.1$.

We would like to point out that we can rewire Eq. (35) as

$$M_{\ell'\ell} \simeq \frac{v}{\sqrt{2}} Y^{\rm eff}_{\ell'\ell}, \tag{38}$$

where

$$Y^{\rm eff}_{\ell'\ell} = Y_{\ell'\ell} \left( \frac{\langle \pi_0 \rangle}{f} \frac{1}{q^j} \right) \tag{39}$$

behaves like *effective clockworked Yukawa couplings*. We can use the clockworked VEVs mechanism to realize the clockworked Yukawa couplings as well as clockworked VEVs.

Because all the flavor indices are assigned to the Yukawa couplings, the structure of the flavor mixings is controlled by the Yukawa couplings $Y_{\ell'\ell}$. The clockwork part $\left( \frac{\langle \pi_0 \rangle}{f} \frac{1}{q^j} \right)$ cannot contribute to the details of the flavor structure; it just guarantees the generation of the tiny neutrino masses even if the magnitudes of the Yukawa couplings are of order one.

### *3.3. Clockwork dominant*

As the opposite of the Yukawa dominant case, if we assume that the Yukawa couplings are extremely democratic [57],

$$|Y_{\ell'\ell}| = 1, \tag{40}$$

then the details of the flavor structure should be controlled by the clockwork part $\left( \frac{\langle \pi_0 \rangle}{f} \frac{1}{q^j} \right)$. In this case, the clockwork part should have the flavor indices $\ell', \ell = e, \mu, \tau$.

Without discussions of the physical possibility of the model building, there are several possible combinations of the assignment of the flavor indices in the clockwork part. For example, there are four possible combinations of the flavor indices $\ell'$ and $\ell$ for $\pi_0$, e.g. $\pi_0^{(\ell'\ell)}$, $\pi_0^{(\ell')}$, $\pi_0^{(\ell)}$, and $\pi_0$. As for $\pi_0$, the other three parameters, $f$, $q$, and $j$, in the clockwork part could be flavored parameters. The total number of assignment combinations of the flavor indices is $4^4 = 256$. The minimum assignment of the flavor indices yields the flavor neutrino masses

$$|M_{\ell'\ell}| = \frac{v}{\sqrt{2}} \frac{\langle \pi_0 \rangle}{f} \frac{1}{q^j}, \tag{41}$$

which is essentially same as the one-flavor neutrino (without mixing) clockworked VEVs case in the previous section. On the other hand, the maximal assignment of the flavor indices yields

$$|M_{\ell'\ell}| = \frac{v}{\sqrt{2}} \frac{\langle \pi_0^{(\ell'\ell)} \rangle}{f_{\ell'\ell}} \frac{1}{q_{\ell'\ell}^{j_{\ell'\ell}}}. \tag{42}$$

Since the conditions $q = 2, 3$ and $j \in \mathbb{N}$ should be satisfied in the one-flavor neutrino clockwork models, we require the condition

$$q_{\ell'\ell} = 2, 3, \qquad j_{\ell'\ell} \in \mathbb{N} \tag{43}$$

in the three neutrino flavor models. With these requirements, we have the constraints on the site number as

$$
\begin{aligned}
j_{\ell'\ell} &= \begin{cases} 36, 37, \ldots, 49 & (q_{\ell'\ell} = 2) \\ 23, 24, \ldots, 31 & (q_{\ell'\ell} = 3) \end{cases} \quad (m_1 = 0.001\,\text{eV}), \\
j_{\ell'\ell} &= \begin{cases} 36, 37, \ldots, 46 & (q_{\ell'\ell} = 2) \\ 23, 24, \ldots, 29 & (q_{\ell'\ell} = 3) \end{cases} \quad (m_1 = 0.01\,\text{eV}), \\
j_{\ell'\ell} &= \begin{cases} 35, 36, \ldots, 43 & (q_{\ell'\ell} = 2) \\ 22, 23, \ldots, 27 & (q_{\ell'\ell} = 3) \end{cases} \quad (m_1 = 0.1\,\text{eV}),
\end{aligned} \tag{44}
$$

for $0.01 \leq \langle \pi_0^{(\ell'\ell)} \rangle / f_{\ell'\ell} \leq 1$ by the relation

$$
j_{\ell'\ell} = \log_{q_{\ell'\ell}} \left( \frac{v}{\sqrt{2}} \frac{\langle \pi_0^{(\ell'\ell)} \rangle}{f_{\ell'\ell}} \frac{1}{|M_{\ell'\ell}|} \right) \tag{45}
$$

and Eq. (30).

Hereafter, the mathematical capability of generating a correct flavor neutrino mass matrix will be discussed for some selected cases.

(I) Single parameter: First, we assume that the flavor structure is controlled by a single model parameter, e.g. only $q$, $j$, $\pi_0$, or $f$ controls the flavor structure. In this case there are only four possible combinations of the flavor indices:

$$
|M_{\ell'\ell}| \propto \begin{cases} \frac{\langle \pi_0 \rangle}{f} \frac{1}{q_{\ell'\ell}^j} & (q_{\ell'\ell}), \\ \frac{\langle \pi_0 \rangle}{f} \frac{1}{q^{j_{\ell'\ell}}} & (j_{\ell'\ell}), \\ \frac{\langle \pi_0^{(\ell'\ell)} \rangle}{f} \frac{1}{q^j} & (\pi_0^{(\ell'\ell)}), \\ \frac{\langle \pi_0 \rangle}{f_{\ell'\ell}} \frac{1}{q^j} & (f_{\ell'\ell}). \end{cases}
$$

These are mathematically, and probably physically, the most simple assignments in this paper. We see that we cannot obtain the correct flavor neutrino mass matrix in the first two cases (the single-flavored $q_{\ell'\ell}$ case and the single-flavored $j_{\ell'\ell}$ case). On the contrary, the correct flavor neutrino mass matrix can be realized in the last two cases (the single-flavored $\pi_0^{(\ell'\ell)}$ case and the single-flavored $f_{\ell'\ell}$ case).

(II) Double parameters: Next, we assume that the flavor structure is controlled by double parameters of the model. Because the single-flavored $q_{\ell'\ell}$ or the single-flavored $j_{\ell'\ell}$ is incapable of generating the correct flavor neutrino mass matrix, we study the effects of collaboration between these two parameters:

$$
|M_{\ell'\ell}| \propto \frac{\langle \pi_0 \rangle}{f} \frac{1}{q_{\ell'\ell}^{j_{\ell'\ell}}} (q_{\ell'\ell} \text{ and } j_{\ell'\ell}). \tag{46}
$$

We show that we cannot obtain the correct flavor neutrino mass matrix in this case. Moreover, since the single-flavored $\pi_0^{(\ell'\ell)}$ and the single-flavored $f_{\ell'\ell}$ are capable of producing the correct flavor neutrino mass matrix, we see whether or not $\pi_0^{(\ell)}$ can assist $q_{\ell'\ell}$ or $j_{\ell'\ell}$ to realize the correct flavor neutrino mass matrix. It will be shown that the following two cases are incapable of generating the correct flavor neutrino mass matrix:

$$|M_{\ell'\ell}| \propto \begin{cases} \frac{\langle \pi_0^{(\ell')} \rangle}{f} \frac{1}{q_{\ell'\ell}^{j}} & (\pi_0^{(\ell')} \text{ and } q_{\ell'\ell}), \\ \frac{\langle \pi_0^{(\ell')} \rangle}{f} \frac{1}{q^{j_{\ell'\ell}}} & (\pi_0^{(\ell')} \text{ and } j_{\ell'\ell}). \end{cases}$$

We see that the other some cases, such as

$$|M_{\ell'\ell}| \propto \frac{\langle \pi_0 \rangle}{f_{\ell'}} \frac{1}{q_{\ell'\ell}^{j}} (f_{\ell'} \text{ and } q_{\ell'\ell}),$$

are also incapable of generating the correct flavor neutrino mass matrix.

(III) Triple parameters: Finally, we assume that the flavor structure is controlled by triple model parameters. As an example of the triple-parameter case, we see whether the flavor neutrino masses

$$|M_{\ell'\ell}| \propto \frac{\langle \pi_0^{(\ell')} \rangle}{f} \frac{1}{q_{\ell'\ell}^{j_{\ell'\ell}}} (\pi_0^{(\ell')},\ q_{\ell'\ell}, \text{ and } j_{\ell'\ell})$$

can be consistent with observations.

Detailed discussion about the capability of generating the correct flavor neutrino mass matrix in these selected cases follow.

### 3.4. (I-1) $q_{\ell'\ell}$ dominant

If the flavor structure is controlled by $q_{\ell'\ell}$, the elements of the flavor neutrino mass matrix become

$$|M_{\ell'\ell}| = \frac{v}{\sqrt{2}} \frac{\langle \pi_0 \rangle}{f} \frac{1}{q_{\ell'\ell}^{j}}. \tag{47}$$

To reproduce the flavor structure of the neutrino sector (the nine elements of the flavor neutrino mass matrix: $M_{ee}, M_{e\mu}, \ldots, M_{\tau\tau}$), at least nine different values of $|M_{\ell'\ell}|$ should be predicted for the fixed $\langle \pi_0 \rangle, f$, and $j$; however, only two different discrete numbers,

$$|M_{\ell'\ell}| = \frac{v}{\sqrt{2}} \frac{\langle \pi_0 \rangle}{f} \times \underbrace{\left\{ \frac{1}{2^j}, \frac{1}{3^j} \right\}}_{\text{2 numbers}}, \tag{48}$$

could be predicted with the requirement of $q_{\ell'\ell} = 2, 3$. We conclude that the $q_{\ell'\ell}$ dominant case is excluded from observations. Thus, the correct flavor neutrino mass matrix cannot be realized in the $q_{\ell'\ell}$ dominant case.

If we relax the requirements of $q_{\ell'\ell} \in \mathbb{N}$ and allow real and positive $q_{\ell'\ell}$, there are many solutions which are consistent with observations. For example,

$$\begin{pmatrix} q_{ee} & q_{e\mu} & q_{e\tau} \\ q_{\mu e} & q_{\mu\mu} & q_{\mu\tau} \\ q_{\tau e} & q_{\tau\mu} & q_{\tau\tau} \end{pmatrix} = \begin{pmatrix} 2.964 & 3.014 & 3.167 \\ 3.036 & 3.029 & 2.963 \\ 3.077 & 2.988 & 2.977 \end{pmatrix} \tag{49}$$

with $\langle \pi_0 \rangle / f = 0.1$ and $j = 24$ yield the flavor neutrino mass matrix in Eq. (29) that is consistent with the best-fit values of the neutrino oscillation parameters for $m_1 = 0.1$ eV.

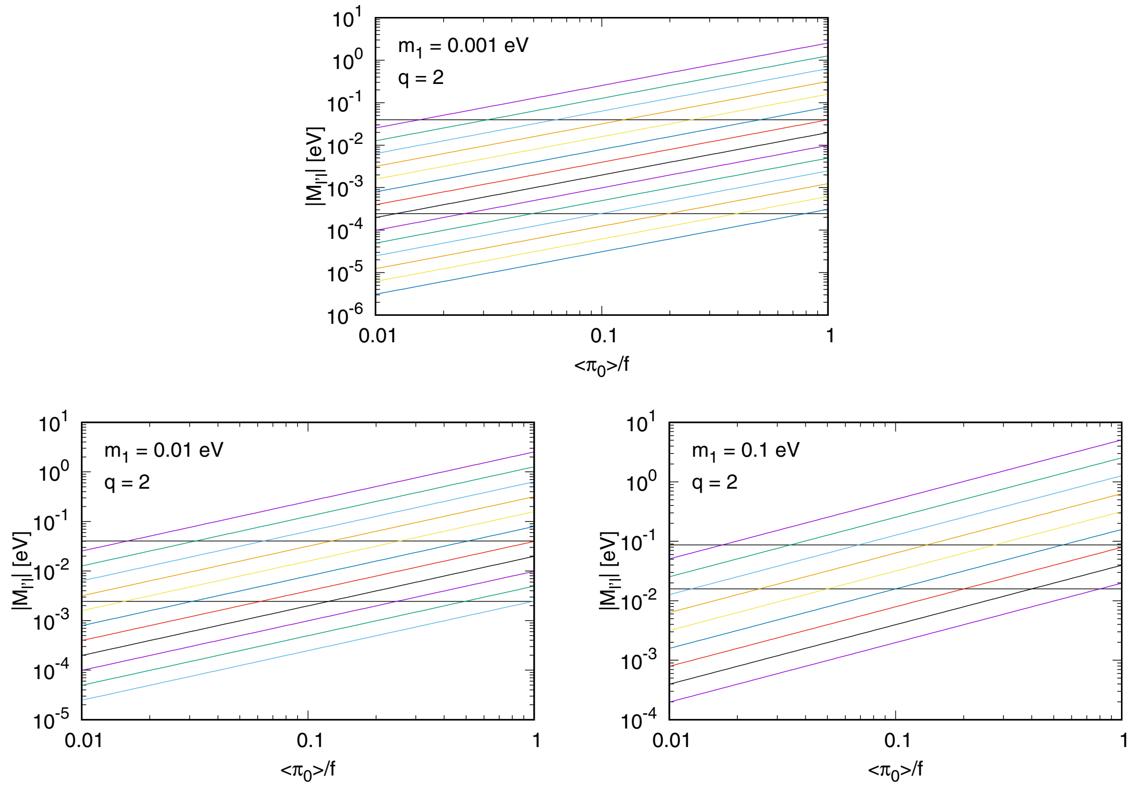


**Fig. 2.** $|M_{\ell'\ell}|$ vs. $\langle\pi_0\rangle/f$ for $q = 2$ in the $j_{\ell'\ell}$ dominant case. In the upper panel, the 14 lines corresponding to $q^{j_{\ell'\ell}} = 2^{36}$ (the upper line), $q^{j_{\ell'\ell}} = 2^{37}$ (next to upper line), to $q^{j_{\ell'\ell}} = 2^{49}$ (the lower line) are shown for $m_1 = 0.001$ eV and $q = 2$. The horizontal lines show the observed upper and lower bounds of the flavor neutrino masses in the $3\sigma$ region. The predicted nine different neutrino masses should be in this $3\sigma$ band; however, there are maximally eight different discrete values of $|M_{\ell'\ell}|$ within the $3\sigma$ band for fixed $\langle\pi_0\rangle/f$. The lower panels are similar, but for $m_1 = 0.01$ eV and $m_1 = 0.1$ eV.

### *3.5. (I-2) $j_{\ell'\ell}$ dominant*

If the flavor structure is controlled by $j_{\ell'\ell}$, the elements of the flavor neutrino mass matrix become

$$|M_{\ell'\ell}| = \frac{v}{\sqrt{2}}\frac{\langle\pi_0\rangle}{f}\frac{1}{q^{j_{\ell'\ell}}}. \tag{50}$$

As for the $q_{\ell'\ell}$ dominant case, at least nine different values of $|M_{\ell'\ell}|$ should be predicted for fixed $\langle\pi_0\rangle/f$ and $q$. Although the 14 discrete values

$$|M_{\ell'\ell}| = \frac{v}{\sqrt{2}}\frac{\langle\pi_0\rangle}{f} \times \underbrace{\left\{\frac{1}{2^{36}}, \frac{1}{2^{37}}, \ldots, \frac{1}{2^{49}}\right\}}_{\text{14 numbers}} \tag{51}$$

could be predicted for $m_1 = 0.001$ eV and $q = 2$, see Eq. (44), these values are inconsistent with observation for the following reason.

Figure 2 shows $|M_{\ell'\ell}|$ vs. $\langle\pi_0\rangle/f$ in the $j_{\ell'\ell}$ dominant case. In the upper panel, the 14 lines corresponding to $q^{j_{\ell'\ell}} = 2^{36}$ (the upper line), $q^{j_{\ell'\ell}} = 2^{37}$ (next to upper line), to $q^{j_{\ell'\ell}} = 2^{49}$ (the lower line) are shown for $m_1 = 0.001$ eV and $q = 2$. The horizontal lines show the observed upper and lower bounds of the flavor neutrino masses for $m_1 = 0.001$ eV in the $3\sigma$ region. The nine different neutrino masses $|M_{ee}|, |M_{e\mu}|, \ldots, |M_{\tau\tau}|$ should be in this $3\sigma$ band; however, there are maximally eight different values of $|M_{\ell'\ell}|$ within the $3\,\sigma$ band for fixed $\langle\pi_0\rangle/f$. For example, we obtain only the eight numbers

$$|M_{\ell'\ell}| = \{0.000247,\ 0.000495,\ 0.000990,\ 0.00198,\ \underbrace{0.00396,\ 0.00792,\ 0.0158,\ 0.0317\}\ \mathrm{eV}}_{8\ \text{numbers}} \tag{52}$$

for $\langle\pi_0\rangle/f = 0.1$. In the case of $m_1 = 0.01$ eV (see the lower-left panel in Fig. 2) we have 11 different discrete values for $q = 2$; however, there are maximally four different values of $|M_{\ell'\ell}|$ within the $3\,\sigma$ band for fixed $\langle\pi_0\rangle/f$. In the case of $m_1 = 0.1$ eV (see the lower-right panel in Fig. 2) we have just nine different discrete values for $q = 2$; however, there are maximally three different values of $|M_{\ell'\ell}|$ within the $3\,\sigma$ band. From similar discussions, it turns out that the predicted flavor neutrino masses for $q = 3$ are also inconsistent with observations. We conclude that the $j_{\ell'\ell}$ dominant case for $0.001\ \mathrm{eV} \le m_1 \le 0.1\ \mathrm{eV}$ and $0.01 \le \langle\pi_0\rangle/f \le 1$ is excluded from the $3\,\sigma$ region of neutrino experiments.

If we relax the requirements of $j_{\ell'\ell} \in \mathbb{N}$ and allow real and positive $j_{\ell'\ell}$, there are many solutions which are consistent with observations. For example,

$$\begin{pmatrix} j_{ee} & j_{e\mu} & j_{e\tau} \\ j_{\mu e} & j_{\mu\mu} & j_{\mu\tau} \\ j_{\tau e} & j_{\tau\mu} & j_{\tau\tau} \end{pmatrix} = \begin{pmatrix} 23.74 & 24.10 & 25.19 \\ 24.26 & 24.21 & 23.73 \\ 24.55 & 23.91 & 23.84 \end{pmatrix} \tag{53}$$

with $\langle\pi_0\rangle/f = 0.1$ and $q = 3$ yield the flavor neutrino mass matrix in Eq. (29) that is consistent with the best-fit values of neutrino oscillation parameters for $m_1 = 0.1$ eV.

### 3.6. *(I-3) $\pi_0^{(\ell'\ell)}$ dominant*

If the flavor structure is controlled by $\langle\pi_0^{(\ell'\ell)}\rangle$, the elements of the neutrino mass matrix become

$$|M_{\ell'\ell}| = \frac{v}{\sqrt{2}}\frac{\langle\pi_0^{(\ell'\ell)}\rangle}{f}\frac{1}{q^j}. \tag{54}$$

In this case, we can obtain flavor neutrino mass matrices which are consistent with observations. For example,

$$\frac{1}{f}\begin{pmatrix} \langle\pi_0^{(ee)}\rangle & \langle\pi_0^{(e\mu)}\rangle & \langle\pi_0^{(e\tau)}\rangle \\ \langle\pi_0^{(\mu e)}\rangle & \langle\pi_0^{(\mu\mu)}\rangle & \langle\pi_0^{(\mu\tau)}\rangle \\ \langle\pi_0^{(\tau e)}\rangle & \langle\pi_0^{(\tau\mu)}\rangle & \langle\pi_0^{(\tau\tau)}\rangle \end{pmatrix} = \begin{pmatrix} 0.1333 & 0.08960 & 0.02715 \\ 0.07483 & 0.07929 & 0.1347 \\ 0.05440 & 0.1104 & 0.1187 \end{pmatrix} \tag{55}$$

with $q = 3$ and $j = 24$ yield the flavor neutrino mass matrix in Eq. (29).

Figure 3 shows $|M_{\ell'\ell}|$ vs. $\langle\pi_0^{(\ell'\ell)}\rangle/f$ for $q^j = 3^{24}$ in the $\langle\pi_0^{(\ell'\ell)}\rangle$ dominated case. The horizontal lines show the observed upper and lower bounds of the flavor neutrino masses in the $3\,\sigma$ region. The nine plus symbols correspond to the nine elements in Eq. (55). We see that the nine different predicted neutrino masses are consistent with observations.

### 3.7. *(I-4) $f_{\ell'\ell}$ dominant*

If the flavor structure is controlled by $f_{\ell'\ell}$, the elements of the neutrino mass matrix become

$$|M_{\ell'\ell}| = \frac{v}{\sqrt{2}}\frac{\langle\pi_0\rangle}{f_{\ell'\ell}}\frac{1}{q^j}. \tag{56}$$

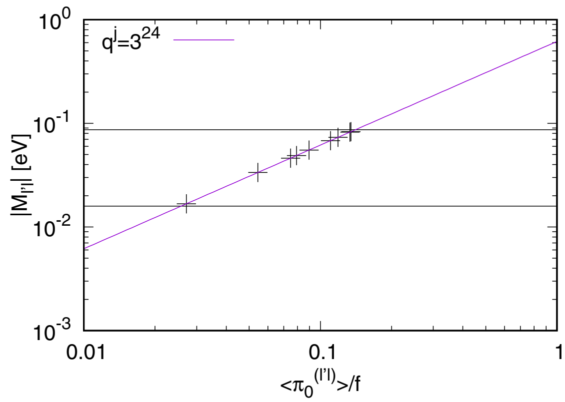


**Fig. 3.** $|M_{\ell'\ell}|$ vs. $\langle\pi_0^{(\ell'\ell)}\rangle/f$ for $q^j = 3^{24}$ in the $\pi_0$ dominated case. The horizontal lines show the observed upper and lower bounds of the flavor neutrino masses in the $3\,\sigma$ region. The nine plus symbols correspond to the nine elements in Eq. (55). The nine different predicted neutrino masses are consistent with observations.

In this case, we have the same conclusion as in the $\pi_0^{(\ell'\ell)}$ dominant case with the replacement

$$\frac{\langle\pi_0^{(\ell'\ell)}\rangle}{f} \to \frac{\langle\pi_0\rangle}{f_{\ell'\ell}} \tag{57}$$

in Eq. (54). Thus, the correct flavor neutrino mass matrix can be realized in the $f_{\ell'\ell}$ dominant case.

### 3.8. *(II-1) $q_{\ell'\ell}$ and $j_{\ell'\ell}$ dominant*

If the flavor structure is controlled by $q_{\ell'\ell}$ and $j_{\ell'\ell}$, the elements of the neutrino mass matrix become

$$|M_{\ell'\ell}| = \frac{v}{\sqrt{2}}\frac{\langle\pi_0\rangle}{f}\frac{1}{q_{\ell'\ell}^{j_{\ell'\ell}}}. \tag{58}$$

As in the $q_{\ell'\ell}$ dominant case, at least nine different values of $|M_{\ell'\ell}|$ should be predicted for fixed $\langle\pi_0\rangle/f$. Although 14 discrete values for $q = 2$ and 9 discrete values for $q = 3$ could be predicted for $m_1 = 0.001$ eV, it turns out that these predicted values of $|M_{ee}|, |M_{e\mu}|, \ldots, |M_{\tau\tau}|$ are inconsistent with Eq. (31) for $\langle\pi_0\rangle/f = 0.01 - 1$. We have similar results for $m_1 = 0.001$–$0.1$ eV. We conclude that the $q_{\ell'\ell}$ and $j_{\ell'\ell}$ dominant case for $0.001\text{ eV} \le m_1 \le 0.1$ eV and $0.01 \le \langle\pi_0\rangle/f \le 1$ is excluded from the $3\,\sigma$ region of the neutrino experiments.

### 3.9. *(II-2) $\pi_0^{(\ell')}$ and $q_{\ell'\ell}$ dominant*

If the flavor structure is controlled by $\pi_0^{(\ell')}$ and $q_{\ell'\ell}$, the elements of the neutrino mass matrix become

$$|M_{\ell'\ell}| = \frac{v}{\sqrt{2}}\frac{\langle\pi_0^{(\ell')}\rangle}{f}\frac{1}{q_{\ell'\ell}^{j}}. \tag{59}$$

To reproduce the three elements of the flavor neutrino mass matrix $M_{\ell'e}$, $M_{\ell'\mu}$, and $M_{\ell'\tau}$, at least three different values of $|M_{\ell'\ell}|$ should be obtained for fixed $f$ and $j$; however, only two different discrete numbers,

$$|M_{\ell'\ell}| = \frac{v}{\sqrt{2}}\frac{\langle\pi_0^{(\ell')}\rangle}{f} \times \underbrace{\left\{\frac{1}{2^j}, \frac{1}{3^j}\right\}}_{\text{2 numbers}}, \tag{60}$$

are obtained with the requirement of $q_{\ell'\ell} = 2, 3$. We conclude that the $\pi_0^{(\ell')}$ and $q_{\ell'\ell}$ dominant case is excluded from observations.

From similar discussions, it turns out that the following assignment of the flavor indices to the flavor neutrino masses,

$$|M_{\ell'\ell}| = \frac{v}{\sqrt{2}} \frac{\langle \pi_0^{(\ell)} \rangle}{f} \frac{1}{q_{\ell'\ell}^{j}} \tag{61}$$

and

$$|M_{\ell'\ell}| = \frac{v}{\sqrt{2}} \frac{\langle \pi_0 \rangle}{f_{\ell'}} \frac{1}{q_{\ell'\ell}^{j}}, \qquad |M_{\ell'\ell}| = \frac{v}{\sqrt{2}} \frac{\langle \pi_0 \rangle}{f_{\ell}} \frac{1}{q_{\ell'\ell}^{j}}, \tag{62}$$

cannot yield the correct flavor neutrino mass matrix.

### 3.10. (II-3) $\pi_0^{(\ell')}$ and $j_{\ell'\ell}$ dominant

If the flavor structure is controlled by $\pi_0^{(\ell')}$ and $j_{\ell'\ell}$, the elements of the neutrino mass matrix become

$$|M_{\ell'\ell}| = \frac{v}{\sqrt{2}} \frac{\langle \pi_0^{(\ell')} \rangle}{f} \frac{1}{q^{j_{\ell'\ell}}}. \tag{63}$$

From discussions similar to the $q_{\ell'\ell}$ and $j_{\ell'\ell}$ dominant case, we conclude that the $\pi_0^{(\ell')}$ and $j_{\ell'\ell}$ dominant case for 0.001 eV $\le m_1 \le$ 0.1 eV and $0.01 \le \langle \pi_0 \rangle / f \le 1$ is excluded from the 3 $\sigma$ region of neutrino experiments.

From similar discussions, it turns out that the flavor neutrino masses

$$|M_{\ell'\ell}| = \frac{v}{\sqrt{2}} \frac{\langle \pi_0^{(\ell)} \rangle}{f} \frac{1}{q^{j_{\ell'\ell}}} \tag{64}$$

and

$$|M_{\ell'\ell}| = \frac{v}{\sqrt{2}} \frac{\langle \pi_0 \rangle}{f_{\ell'}} \frac{1}{q^{j_{\ell'\ell}}}, \qquad |M_{\ell'\ell}| = \frac{v}{\sqrt{2}} \frac{\langle \pi_0 \rangle}{f_{\ell}} \frac{1}{q^{j_{\ell'\ell}}} \tag{65}$$

are also inconsistent with observations.

### 3.11. (III) $\pi_0^{(\ell')}$, $q_{\ell'\ell}$, and $j_{\ell'\ell}$ dominant

If the flavor structure is controlled by $\pi_0^{(\ell')}$, $q_{\ell'\ell}$, and $j_{\ell'\ell}$, the elements of the neutrino mass matrix become

$$|M_{\ell'\ell}| = \frac{v}{\sqrt{2}} \frac{\langle \pi_0^{(\ell')} \rangle}{f} \frac{1}{q_{\ell'\ell}^{j_{\ell'\ell}}}. \tag{66}$$

In this case, we can obtain flavor neutrino mass matrices which are consistent with observations. For example,

$$\frac{1}{f} \begin{pmatrix} \frac{\langle \pi_0^{(e)} \rangle}{q_{ee}^{j_{ee}}} & \frac{\langle \pi_0^{(e)} \rangle}{q_{e\mu}^{j_{e\mu}}} & \frac{\langle \pi_0^{(e)} \rangle}{q_{e\tau}^{j_{e\tau}}} \\ \frac{\langle \pi_0^{(\mu)} \rangle}{q_{\mu e}^{j_{\mu e}}} & \frac{\langle \pi_0^{(\mu)} \rangle}{q_{\mu\mu}^{j_{\mu\mu}}} & \frac{\langle \pi_0^{(\mu)} \rangle}{q_{\mu\tau}^{j_{\mu\tau}}} \\ \frac{\langle \pi_0^{(\tau)} \rangle}{q_{\tau e}^{j_{\tau e}}} & \frac{\langle \pi_0^{(\tau)} \rangle}{q_{\tau\mu}^{j_{\tau\mu}}} & \frac{\langle \pi_0^{(\tau)} \rangle}{q_{\tau\tau}^{j_{\tau\tau}}} \end{pmatrix} = \begin{pmatrix} \frac{0.35}{3^{27}} & \frac{0.35}{2^{43}} & \frac{0.35}{3^{27}} \\ \frac{0.25}{2^{43}} & \frac{0.25}{3^{27}} & \frac{0.25}{2^{40}} \\ \frac{0.4}{3^{28}} & \frac{0.4}{2^{43}} & \frac{0.4}{2^{41}} \end{pmatrix} \tag{67}$$

yields the following magnitude of the flavor neutrino mass matrix,

$$\begin{pmatrix} |M_{ee}| & |M_{e\mu}| & |M_{e\tau}| \\ |M_{\mu e}| & |M_{\mu\mu}| & |M_{\mu\tau}| \\ |M_{\tau e}| & |M_{\tau\mu}| & |M_{\tau\tau}| \end{pmatrix} = \begin{pmatrix} 0.00799 & 0.00693 & 0.00780 \\ 0.00495 & 0.00571 & 0.0396 \\ 0.00304 & 0.00792 & 0.0317 \end{pmatrix} \text{eV}, \tag{68}$$

which is consistent with observations in the $3\,\sigma$ region—see Eq. (32).

Moreover, the flavor neutrino masses

$$|M_{\ell'\ell}| = \frac{v}{\sqrt{2}} \frac{\langle \pi_0^{(\ell)} \rangle}{f} \frac{1}{q_{\ell'\ell}^{j_{\ell'\ell}}} \tag{69}$$

are also consistent with observations. For example,

$$\frac{1}{f} \begin{pmatrix} \frac{\langle \pi_0^{(e)} \rangle}{q_{ee}^{j_{ee}}} & \frac{\langle \pi_0^{(\mu)} \rangle}{q_{e\mu}^{j_{e\mu}}} & \frac{\langle \pi_0^{(\tau)} \rangle}{q_{e\tau}^{j_{e\tau}}} \\ \frac{\langle \pi_0^{(e)} \rangle}{q_{\mu e}^{j_{\mu e}}} & \frac{\langle \pi_0^{(\mu)} \rangle}{q_{\mu\mu}^{j_{\mu\mu}}} & \frac{\langle \pi_0^{(\tau)} \rangle}{q_{\mu\tau}^{j_{\mu\tau}}} \\ \frac{\langle \pi_0^{(e)} \rangle}{q_{\tau e}^{j_{\tau e}}} & \frac{\langle \pi_0^{(\mu)} \rangle}{q_{\tau\mu}^{j_{\tau\mu}}} & \frac{\langle \pi_0^{(\tau)} \rangle}{q_{\tau\tau}^{j_{\tau\tau}}} \end{pmatrix} = \begin{pmatrix} \frac{0.12}{3^{26}} & \frac{0.1}{3^{26}} & \frac{0.11}{3^{26}} \\ \frac{0.12}{2^{42}} & \frac{0.1}{2^{41}} & \frac{0.11}{2^{39}} \\ \frac{0.12}{3^{27}} & \frac{0.1}{2^{41}} & \frac{0.11}{2^{39}} \end{pmatrix} \tag{70}$$

yields

$$\begin{pmatrix} |M_{ee}| & |M_{e\mu}| & |M_{e\tau}| \\ |M_{\mu e}| & |M_{\mu\mu}| & |M_{\mu\tau}| \\ |M_{\tau e}| & |M_{\tau\mu}| & |M_{\tau\tau}| \end{pmatrix} = \begin{pmatrix} 0.00822 & 0.00685 & 0.00753 \\ 0.00475 & 0.00792 & 0.0348 \\ 0.00274 & 0.00792 & 0.0348 \end{pmatrix} \text{eV}, \tag{71}$$

which is consistent with Eq. (32).

## 4. Summary

The clockwork mechanism provides a natural way to obtain the hierarchical masses and couplings in a theory. In previous studies there are fermion clockwork models for the neutrino mixings; however, there is no scalar clockwork model for the neutrino mixings. In this paper, towards a construction of scalar clockwork models including neutrino mixings, we have studied the mathematical capability of generating the correct flavor neutrino mass matrix in a scalar clockwork model.

First, we assumed that the flavor structure is controlled by the Yukawa couplings. In this case, we can obtain the correct flavor neutrino mass matrix by appropriate Yukawa couplings $Y_{\ell'\ell}$ where $\ell', \ell = e, \mu, \tau$.

Next, we assumed that the Yukawa couplings are extremely democratic $|Y_{\ell'\ell}| = 1$. In this case, the clockwork part $\left(\frac{\langle \pi_0 \rangle}{f} \frac{1}{q^j}\right)$ should have the flavor indices $\ell'$ and $\ell$. We found that if the flavor structure is controlled by single-flavored parameter $\langle \pi_0^{(\ell'\ell)} \rangle$ or $f_{\ell'\ell}$ in a scalar clockwork model, there is the mathematical capability of generating the correct flavor mass matrix in the model. In addition, if the flavor structure is controlled by triple-flavored parameters, $\pi_0^{(\ell')}$, $q_{\ell'\ell}$, and $j_{\ell'\ell}$, in a scalar clockwork model, the predicted flavor neutrino mass matrix can be consistent with observation in the $3\,\sigma$ region.

Although, we have acheived the main goal of our discussions to see the mathematical capability of generating the correct flavor neutrino mass matrix in a scalar clockwork model, an additional discussion to see the physical availability of the model building may be required to confirm the results of our discussion. Hereafter, we will show three toy models for neutrino mixings in the scalar clockwork schemes (we would like to discuss the details of the model building and phenomenological consequences such as collider experiments as a separate work in the future).

### *4.1.* $\pi_0^{(\ell'\ell)}$ *dominant case*

First, we show a toy model for the $\pi_0^{(\ell'\ell)}$ dominant case (see Sect. 3.6). In this case, to realize the *ee* element of the flavor neutrino mass matrix,

$$|M_{ee}| = \frac{v}{\sqrt{2}} \frac{\langle \pi_0^{(ee)} \rangle}{f} \frac{1}{q^j}, \tag{72}$$

the clockwork chain

$$\begin{array}{c} \langle \pi_0^{(ee)} \rangle - \dfrac{\langle \pi_0^{(ee)} \rangle}{q} - \cdots - \dfrac{\langle \pi_0^{(ee)} \rangle}{q^j} - \cdots - \dfrac{\langle \pi_0^{(ee)} \rangle}{q^N} \\ \qquad\qquad\qquad | \\ \qquad\qquad\qquad \nu_{eR}^{(e)} \end{array} \tag{73}$$

is required. In addition to this chain, another eight chains for $|M_{e\mu}|, |M_{e\tau}|, \ldots, |M_{\tau\tau}|$ are required. Therefore, a new scalar clockwork model that has nine clockwork chains in the clockwork sector is required to predict the nine flavor neutrino masses in the $\pi_0^{(\ell'\ell)}$ dominant case. A candidate for the Lagrangian of this model is

$$\mathcal{L}_{\mathrm{SM-CW}} = \sum_{\ell',\ell} Y_{\ell'\ell} \left( \frac{\pi_j^{(\ell'\ell)}}{f} \right) \bar{\ell}'_L \tilde{H} \nu_{\ell R}^{(\ell')} + \text{h.c.} \tag{74}$$

There are nine right-handed neutrinos in this model. Three of these, $\left\{\nu_{eR}^{(e)}, \nu_{\mu R}^{(e)}, \nu_{\tau R}^{(e)}\right\}$, should interact with only the left-handed electron neutrino $\nu_{eL}$ to produce $|M_{ee}|$, $|M_{e\mu}|$, and $|M_{e\tau}|$. Also, $\left\{\nu_{eR}^{(e)}, \nu_{\mu R}^{(e)}, \nu_{\tau R}^{(e)}\right\}$ and $\left\{\nu_{eR}^{(e)}, \nu_{\mu R}^{(e)}, \nu_{\tau R}^{(e)}\right\}$ should interact with only $\nu_{\mu L}$ and $\nu_{\tau L}$, respectively. These specific selections of the couplings might be realized by the flavored clockwork mechanism [43] or assignment of the lepton number to the clockwork sector [52].

Unfortunately, this $\pi_0^{(\ell'\ell)}$ dominant model is complex. While the observed mass matrix can be reproduced, nine clockwork chains (meaning hundreds of extra scalar fields) are introduced to generate the nine elements of the $3 \times 3$ mass matrix, with assumptions on their parameters and their relations (e.g. equality of some of the parameters for all chains). The main cause of this complexity, the nine clockwork chains, in this $\pi_0^{(\ell'\ell)}$ dominant model is our assumption about the number of coupled neutrinos in a clockwork chain. In this toy model we assume that only one neutrino flavor is permitted to couple to one clockwork chain.

A more interesting model may be achieved if different generations of neutrinos couple to different sites in a clockwork chain, which can generate hierarchies between their masses.

### *4.2.* $\pi_0^{(\ell')}$*,* $q_{\ell'\ell}$*, and* $j_{\ell'\ell}$ *dominant case*

Next, we show a toy model for the $\pi_0^{(\ell')}$, $q_{\ell'\ell}$, and $j_{\ell'\ell}$ dominant case (see Sect. 3.11). In this case, for the $ee$, $e\mu$, and $e\tau$ elements of the flavor neutrino mass matrix,

$$|M_{e\ell}| = \frac{v}{\sqrt{2}} \frac{\langle \pi_0^{(e)} \rangle}{f} \frac{1}{q_{e\ell}^{j_{e\ell}}}, \tag{75}$$

a clockwork chain

$$\begin{array}{ccccccccccc} \langle\pi_0^{(e)}\rangle - \cdots - & \dfrac{\langle\pi_0^{(e)}\rangle}{q_{ee}^{j_{ee}}} & - \cdots - & \dfrac{\langle\pi_0^{(e)}\rangle}{q_{e\mu}^{j_{e\mu}}} & - \cdots - & \dfrac{\langle\pi_0^{(e)}\rangle}{q_{e\tau}^{j_{e\tau}}} & - \cdots \\ & | & & | & & | & \\ & \nu_{eR}^{(e)} & & \nu_{\tau R}^{(e)} & & \nu_{\tau R}^{(e)} & \end{array} \tag{76}$$

is required. In addition to the chain in Eq. (76), another two chains for $\left|M_{\mu\ell}\right|$ and $|M_{\tau\ell}|$ are required. Therefore, there are three clockwork chains in the clockwork sector in this model. A candidate for the Lagrangian of this model is

$$\mathcal{L}_{\mathrm{SM-CW}} = \sum_{\ell',\ell} Y_{\ell'\ell} \left( \frac{\pi_{j_{\ell'\ell}}^{(\ell')}}{f} \right) \bar{\ell}'_L \tilde{H} \nu_{\ell R}^{(\ell')} + \mathrm{h.c.} \tag{77}$$

The theoretical origin of inequalities in $q_{\ell'\ell}$ in the same chain may be obtained by non-uniform clockwork schemes (see, for examples, Refs. [50,58]).

### 4.3. $q_{\ell'\ell}$ or $j_{\ell'\ell}$ dominant case

Finally, we show a toy model for the $q_{\ell'\ell}$ or $j_{\ell'\ell}$ dominant cases (see Sects. 3.4 and 3.5). As we mentioned, the correct flavor neutrino mass matrix can be realized in these two cases if the requirements of $q \in \mathbb{N}$ and $j \in \mathbb{N}$ are relaxed in the analysis. In these cases, the correct flavor neutrino mass matrix can be realized as

$$|M_{\ell'\ell}| = \frac{v}{\sqrt{2}} \frac{\langle\pi_0\rangle}{f} \frac{1}{q_{\ell'\ell}^{j}} \tag{78}$$

in the $q_{\ell'\ell}$ dominant case or

$$|M_{\ell'\ell}| = \frac{v}{\sqrt{2}} \frac{\langle\pi_0\rangle}{f} \frac{1}{q^{j_{\ell'\ell}}} \tag{79}$$

in the $j_{\ell'\ell}$ dominant case with only one clockwork chain. A candidate for the Lagrangian of both models is

$$\mathcal{L}_{\mathrm{SM-CW}} = \sum_{\ell',\ell} Y_{\ell'\ell} \left( \frac{\pi_{j_{\ell'\ell}}}{f} \right) \bar{\ell}'_L \tilde{H} \nu_{\ell R}^{(\ell')} + \mathrm{h.c.} \tag{80}$$

A possible candidate for the theoretical origin of continuous $q$ as well as continuous $j$ may be in continuum clockwork schemes [18,59–61]. In this paper we have discussed the capability of generating the correct flavor neutrino mass matrix in the discrete scalar clockwork framework. Constructing a continuum scalar clockwork model for neutrino flavor mixings with only one clockwork chain may be interesting and may appear in future work.

### 4.4. Gauge hierarchy

Finally, we would like to comment on the issue of gauge hierarchy in the context of scalar clockwork. The electroweak scale $v$ is more than 16 orders of magnitude smaller than the Planck scale $M_{\mathrm{pl}}$ in gravity. Within any unified theory of all interactions the small ratio $v/M_{\mathrm{pl}}$ calls for an explanation. Why is the Higgs mass so much smaller than the Planck scale? This is the gauge hierarchy problem

[62,63]. (One of the solutions to the gauge hierarchy problem is realized by introducing the relaxion into the theories [64]. The clockwork mechanisms were originally introduced in the context of weak-scale relaxation [21,22]). Unlike fermionic clockwork, once a large number of scalars are utilized, each of these scalars would appear to have a hierarchy problem: why are their mass scales below the Planck scale? In the context of neutrino mass generation, the scale may be close enough to the Planck scale and the additional hierarchy problems are not severe.

**Funding**

Open Access funding: SCOAP[3].

## References

[1] S. F. King, J. Phys. G: Nucl. Part. Phys. **42**, 123001 (2015).
[2] P. Minkowski, Phys. Lett. B **67**, 421 (1977).
[3] T. Yanagida, Proc. Workshop on Unified Theories and Baryon Number in the Universe, p. 95 (1979).
[4] M. Gell-Mann, P. Ramond, and R. Slansky, in *Supergravity*, eds. P. van Nieuwenhuizen and D. Z. Freedmann (North-Holland, Amsterdam, 1979), p. 315.
[5] R. N. Mohapatra and G. Senjanović, Phys. Rev. Lett. **44**, 912 (1980).
[6] A. Zee, Phys. Lett. B **93**, 389 (1980).
[7] L. Wolfenstein, Nucl. Phys. B **175**, 93 (1980).
[8] S. T. Petcov, Phys. Lett. B **115**, 401 (1982).
[9] A. Zee, Phys. Lett. B **161**, 141 (1985).
[10] A. Zee, Nucl. Phys. B **264**, 99 (1986).
[11] K. S. Babu, Phys. Lett. B **203**, 132 (1988).
[12] D. Chang, W.-Y. Keung, and P. B. Pal, Phys. Rev. Lett. **61**, 2420 (1988).
[13] J. T. Peltoniemi, A. Yu. Smirnov, and J. W. F. Valle, Phys. Lett. B **286**, 321 (1992).
[14] E. Ma, Phys. Rev. D **73**, 077301 (2006).
[15] G. Altarelli and F. Feruglio, Rev. Mod. Phys. **82**, 2701 (2010).
[16] S. F. King and C. Luhn, Rep. Prog. Phys. **76**, 056201 (2013).
[17] Z.-Z. Xing and Z.-H. Zhao, Rep. Prog. Phys. **79**, 076201 (2016).
[18] G. F. Giudice and M. McCullough, J. High Energy Phys. **1702**, 036 (2017).
[19] D. Teresi, arXiv:1705.09698 [hep-ph] [Search INSPIRE].
[20] K. Choi, H. Kim, and S. Yun, Phys. Rev. D **90**, 023545 (2014).
[21] K. Choi and S. H. Im, J. High Energy Phys. **1601**, 149 (2016).
[22] D. E. Kaplan and R. Rattazzi, Phys. Rev. D **93**, 085007 (2016).
[23] M. Farina, D. Pappadopulo, F. Rompineve, and A. Tesi, J. High Energy Phys. **1701**, 095 (2017).
[24] R Coy, M. Frigerio, and M. Ibe, J. High Energy Phys. **1710**, 002 (2017).
[25] P. Agrawal, J. Fan, M. Reece, and L.-T. Wang, J. High Energy Phys. **1802**, 006 (2018).
[26] A. J. Long, J. High Energy Phys. **1807**, 066 (2018).
[27] P. Agrawal, J. Fan, and M. Reece, J. High Energy Phys. **1810**, 193 (2018).
[28] Q. Bonnefoy, E. Dudas, and S. Pokorski, Eur. Phys. J. C **79**, 31 (2019).
[29] K. J. Bae, J. Kost, and C. S. Shin, Phys. Rev. D **99**, 043502 (2019).
[30] A. Kehagias and A. Riotto, Phys. Lett. B **767**, 73 (2017).
[31] S. C. Park and C. S. Shin, Eur. Phys. J. C **79**, 529 (2019).
[32] T. Hambey, D. Teresi, and M. H. G. Tytgat, J. High Energy Phys. **1707**, 047 (2017).
[33] L. Marzola, M. Raidal, and F. R. Urban, Phys. Rev. D **97**, 024010 (2018).
[34] J. Kim and J. McDonald, Phys. Rev. D **98**, 023533 (2018).
[35] A. Goudelis, K. A. Mohan, and D. Sengupta, J. High Energy Phys. **1810**, 014 (2018).
[36] J. Kim and J. McDonald, Phys. Rev. D **98**, 123503 (2018).
[37] D. K. Hong, D. H. Kim, and C. S. Shin, Phys. Rev. D **97**, 035014 (2018).
[38] L. E. Ibáñez and M. Montero, J. High Energy Phys. **1802**, 057 (2018).
[39] I. Antoniadis, A. Delgado, C. Markou, and S. Pokorski, Eur. Phys. J. C **78**, 146 (2018).
[40] S. H. Im, H. P. Hilles, and M. Olechowski, J. High Energy Phys. **1901**, 151 (2019).
[41] A. Kehagias and A. Riotto, J. High Energy Phys. **1802**, 160 (2018).

[42] F. Niedermann, A. Padilla, and P. M. Saffin, Phys. Rev. D **98**, 104014 (2018).
[43] K. M. Patel, Phys. Rev. D **96**, 115013 (2017).
[44] G. von Gersdorff, arXiv:2005.14207 [hep-ph] [Search INSPIRE].
[45] K. S. Babu and S. Saad, arXiv:2007.16085 [hep-ph] [Search INSPIRE].
[46] R. Alonso, A. Carmona, B. M. Dillon, J. F. Kamenik, J. M. Camalich, and J. Zupan, J. High Energy Phys. **1810**, 099 (2018).
[47] A. Ahmed and B. M. Dillon, Phys. Rev. D **96**, 115031 (2017).
[48] S. C. Park and C. S. Shin, Phys. Lett. B **776**, 222 (2018).
[49] A. Banerjee, S. Ghosh, and T. S. Ray, J. High Energy Phys. **1811**, 075 (2018).
[50] S. Hong, G. Kurup, and M. Perelstein, J. High Energy Phys. **1910**, 073 (2019).
[51] A. Ibarra, A. Kushwaha, and S. K. Vempati, Phys. Lett. B **780**, 86 (2018).
[52] T. Kitabayashi, Phys. Rev. D **100**, 035019 (2019).
[53] M. Tanabashi et al. [Particle Data Group], Phys. Rev. D **98**, 030001 (2018).
[54] P. F. de Salas, D. V. Forero, C. A. Ternes, M. Tórtola, and J. W. F. Valle, Phys. Lett. B **782**, 633 (2018).
[55] M. G. Aartsen, et al. [IceCube-Gen2 and JUNO Collaborations], Phys. Rev. D **101**, 032006 (2020).
[56] I. Esteban, M. C. Gonzalez-Garcia, A. Hernandez-Cabezudo, M. Maltoni, and T. Schwetz, J. High Energy Phys. **1901**, 106 (2019).
[57] G. von Gersdorff, J. High Energy Phys. **1709**, 094 (2017).
[58] I. Ben-Dayan, Phys. Rev. D **99**, 096006 (2019).
[59] N. Craig, I. G. Garcia, and D. Sutherland, J. High Energy Phys. **1710**, 018 (2017).
[60] G. F. Giudice, Y. Kats, M. McCullough, R. Torre, and A. Urbano, J. High Energy Phys. **1806**, 009 (2018).
[61] K. Choi, S. H. Im, and C. S. Shin, J. High Energy Phys. **1807**, 113 (2018).
[62] E. Gildener, Phys. Rev. D **14**, 1667 (1976).
[63] S. Weinberg, Phys. Lett. B **82**, 387 (1979).
[64] P. W. Graham, D. E. Kaplan, and S. Rajendran, Phys. Rev. Lett. **115**, 221801 (2015).